

# Effect of spacer layer thickness on the magnetic and magnetotransport properties of $\text{Fe}_3\text{O}_4/\text{Cu}/\text{Ni}_{80}\text{Fe}_{20}$ spin valve structures

D. Tripathy and A. O. Adeyeye\*

*Information Storage Materials Laboratory, Department of Electrical and Computer Engineering,  
National University of Singapore, Singapore 117576*

S. Shannigrahi

*Institute of Materials Research and Engineering, 3 Research Link, Singapore 117602*

(Received 20 June 2006; revised manuscript received 24 September 2006; published 16 January 2007)

We present a systematic and detailed study of the magnetization reversal process and magnetotransport properties of  $\text{Fe}_3\text{O}_4/\text{Cu}$  ( $t_{\text{Cu}}$ )/ $\text{Ni}_{80}\text{Fe}_{20}$  spin valve structures. A drastic change was observed in both the magnetic and transport properties as the thickness of the Cu spacer layer  $t_{\text{Cu}}$  was varied in the range  $2 \text{ nm} \leq t_{\text{Cu}} \leq 30 \text{ nm}$ . For  $t_{\text{Cu}}=2 \text{ nm}$ , the transport properties are mainly due to anisotropic magnetoresistance effects because of strong exchange coupling between the  $\text{Ni}_{80}\text{Fe}_{20}$  and  $\text{Fe}_3\text{O}_4$  layers. For  $t_{\text{Cu}} \geq 5 \text{ nm}$ , however, the transport properties are dominated by positive giant magnetoresistance (GMR) effects due to separate magnetization switching of the two magnetic layers. The GMR ratio decreases with increasing spacer layer thickness due to enhanced current shunting and scattering effects. We also observed that the GMR ratio has strong temperature dependence and decreases with increasing temperature due to spin flip scattering and electron-magnon interactions.

DOI: 10.1103/PhysRevB.75.012403

PACS number(s): 75.70.-i, 75.70.Cn, 75.60.Jk

The magnetic and transport properties of ferromagnetic multilayered systems have garnered intense research activity in recent years not only from a fundamental viewpoint, but also because of its technological relevance to the scientifically rich field of spintronics. Spin-dependent phenomena such as giant magnetoresistance (GMR),<sup>1</sup> and tunneling magnetoresistance (TMR),<sup>2</sup> are promising for application in future spintronic devices like read-out heads in high density magnetic recording and magnetic random access memory (MRAM). The need to improve spin interaction in magnetoresistive systems, and thus increase MR ratio has led to great interest in highly spin polarized ferromagnetic materials such as half metals which they have electrons at the fermi level  $E_F$  in a single spin state.<sup>3</sup> One such half metal is magnetite ( $\text{Fe}_3\text{O}_4$ ), which has been the focus of recent studies due to its high Curie temperature of 858 K and the prediction that it exhibits full negative spin polarization.<sup>4,5</sup>

Recently, some rigorous research has been dedicated towards experimentally investigating the magnetic and transport properties of spin valve structures with half metallic  $\text{Fe}_3\text{O}_4$  inserted as one of the ferromagnetic layers. In a study by Kida *et al.*,<sup>6</sup> the current-in-plane (CIP) MR of  $\text{Co}/\text{Cu}/\text{Fe}_3\text{O}_4$  trilayer films was investigated and a positive GMR ratio of 0.1% was observed at room temperature, which increased to 0.7% at 4.2 K. Positive GMR effect has also been observed in epitaxial trilayers consisting of two different ferrimagnetic layers,  $\text{Fe}_3\text{O}_4$  and  $\text{CoFe}_2\text{O}_4$  separated by a nonmagnetic Au or Pt layer.<sup>7,8</sup> In contrast, a negative GMR was observed for  $\text{Fe}_3\text{O}_4/\text{Au}/\text{Fe}$  spin valve structures measured in the CIP geometry.<sup>9,10</sup> The authors attribute this negative GMR to electrical current being transported through the low resistance Au and Fe layers which results in inverse spin scattering asymmetry at or in the vicinity of the  $\text{Fe}_3\text{O}_4/\text{Au}$  interface. In another work, Takahashi *et al.*<sup>11</sup> have measured the current-perpendicular-to-plane (CPP) MR of

$\text{Ni}_{80}\text{Fe}_{20}/\text{Au}/\text{Fe}_3\text{O}_4$  spin valve trilayers observed a positive GMR ratio which decreases with increasing  $\text{Fe}_3\text{O}_4$  layer thickness. A detailed study of the influence of varying spacer layer thickness on the magnetization reversal process and GMR effect in  $\text{Fe}_3\text{O}_4$  based spin valve structures at various temperatures is however essential for a comprehensive understanding of such structures.

In this work, we have carried out a systematic experimental study of the magnetic and magnetotransport behavior of spin valve structures consisting of  $\text{Ni}_{80}\text{Fe}_{20}$  and  $\text{Fe}_3\text{O}_4$  layers separated by a nonmagnetic Cu spacer layer of varying thickness as a function of temperature.

The  $\text{Fe}_3\text{O}_4/\text{Cu}/\text{Ni}_{80}\text{Fe}_{20}$  spin valve structures were grown on Si(100) substrates by dc magnetron sputtering. The base pressure of the chamber was better than  $3 \times 10^{-8}$  Torr before deposition. The  $\text{Fe}_3\text{O}_4$  film was reactively sputtered at room temperature from a pure Fe target in  $\text{Ar}+\text{O}_2$  mixture. After deposition, the  $\text{Fe}_3\text{O}_4$  layer was annealed at 300 °C for 60 min to remove phases of paramagnetic FeO which may have been formed during reactive sputtering of Fe.<sup>12</sup> The Cu and  $\text{Ni}_{80}\text{Fe}_{20}$  layers were subsequently deposited at room temperature without breaking the vacuum. Phase identification of the films was examined by conventional  $\theta$ - $2\theta$  x-ray diffraction (XRD) scans using Cu  $K\alpha$  radiation. Magnetic properties were characterized using vibrating sample magnetometer (VSM). Electrical contacts to the spin valve structures were made using standard optical lithography, metallization of 200 nm Al, followed by lift off in acetone. The magnetotransport properties of the spin valves were measured as a function of temperature using the standard four probe dc technique in the CIP configuration.

Figure 1 shows a direct comparison of the  $\theta$ - $2\theta$  XRD scans of the  $\text{Fe}_3\text{O}_4/\text{Cu}/\text{Ni}_{80}\text{Fe}_{20}$  spin valve structures as a function of Cu spacer layer thickness. For  $t_{\text{Cu}}=2 \text{ nm}$ , the XRD scans show distinct  $\text{Fe}_3\text{O}_4$  peaks in the (311) and (511)

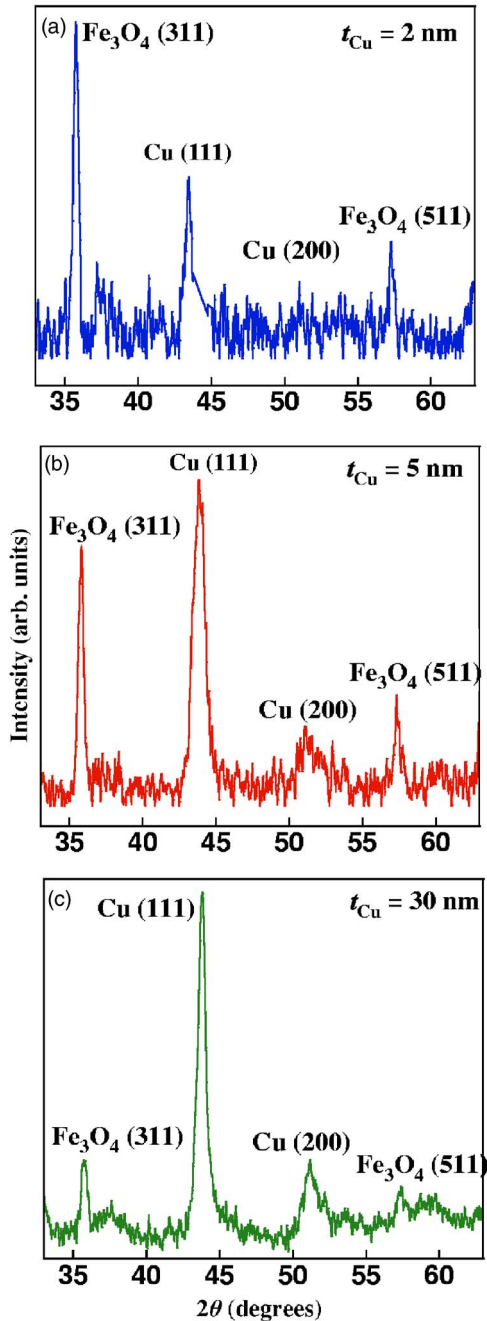


FIG. 1. (Color online). X-ray diffraction patterns for  $\text{Fe}_3\text{O}_4$  (60 nm)/Cu ( $t_{\text{Cu}}$ )/ $\text{Ni}_{80}\text{Fe}_{20}$  (15 nm) spin valve structures at (a)  $t_{\text{Cu}}=2$  nm, (b)  $t_{\text{Cu}}=10$  nm, and (c)  $t_{\text{Cu}}=30$  nm.

orientations. The XRD results clearly show that identical  $\text{Fe}_3\text{O}_4$  peaks are observed for all spacer layer thicknesses. A well defined (111) crystal orientation for the Cu spacer layer was observed in all the spin valve structures. In addition, a small reflection is also observed for the (200) orientation. No clear  $\text{Ni}_{80}\text{Fe}_{20}$  peaks are observed for all structures, indicating that the  $\text{Ni}_{80}\text{Fe}_{20}$  layer grows without a well defined crystal orientation.

Shown in Fig. 2 are the representative in-plane magnetization curves and the corresponding longitudinal magnetoresistance (MR) curves for the  $\text{Fe}_3\text{O}_4/\text{Cu}$  ( $t_{\text{Cu}}$ )/ $\text{Ni}_{80}\text{Fe}_{20}$  trilayer structure measured at room temperature. We ob-

served that the magnetization and MR curves are markedly sensitive to the Cu spacer layer thickness due to interplay of various coupling mechanisms between the  $\text{Ni}_{80}\text{Fe}_{20}$  and  $\text{Fe}_3\text{O}_4$  layers. As shown in Fig. 2(a), magnetizations of the  $\text{Ni}_{80}\text{Fe}_{20}$  and  $\text{Fe}_3\text{O}_4$  layers nearly switch in unison due to strong interlayer exchange coupling between the two magnetic layers for  $t_{\text{Cu}}=2$  nm. This coupling prevents independent magnetization reversal in spite of the difference in coercivity between the two layers. The magnetic moments of the  $\text{Ni}_{80}\text{Fe}_{20}$  and  $\text{Fe}_3\text{O}_4$  layers thus remain parallel as the applied field was swept from positive saturation field to negative saturation field at a constant rate. The strong ferromagnetic coupling may be possibly due to pinholes, which give rise to magnetic bridges through the nonmagnetic Cu spacer layer.<sup>13</sup> It may also be attributed to “orange peel” coupling, which occurs when the surfaces of the sputtered layers are not completely flat. This results in a flux crossover from magnetic poles on one magnetic layer to the poles on the other layer thereby strengthening the ferromagnetic coupling between the  $\text{Ni}_{80}\text{Fe}_{20}$  and  $\text{Fe}_3\text{O}_4$  layers.<sup>14</sup> As expected, the strong interlayer exchange coupling results in MR behavior which is consistent with a typical anisotropic magnetoresistance (AMR) response which is given by<sup>15</sup>

$$R(H) = R_0 + \Delta R \cos^2 \alpha, \quad (1)$$

where  $\alpha$  is the angle between current and magnetization, and  $\Delta R$  signifies the AMR effect.

As  $t_{\text{Cu}}$  increases, the strength of interlayer exchange coupling between the magnetic layers decreases rapidly. For  $t_{\text{Cu}}=5$  nm, the magnetization curve exhibits a clear two-step magnetization reversal process corresponding to switching of the soft  $\text{Ni}_{80}\text{Fe}_{20}$  layer at low magnetic field, followed by a gradual switching of the hard  $\text{Fe}_3\text{O}_4$  layer at a higher field. The MR curves also exhibit marked modification for  $t_{\text{Cu}} \geq 5$  nm and are characterized by the superposition of AMR and GMR effects. The small AMR effect is primarily due to magnetization reversal in the  $\text{Ni}_{80}\text{Fe}_{20}$  layer, through which part of the in-plane electrical sense current is being transported, while the positive GMR effect is due to separate magnetization reversal of the  $\text{Ni}_{80}\text{Fe}_{20}$  and  $\text{Fe}_3\text{O}_4$  layers. As shown in Fig. 2(b)–2(d), the detailed features of the MR curves are strongly dependent on  $t_{\text{Cu}}$ . The interlayer exchange coupling between the  $\text{Ni}_{80}\text{Fe}_{20}$  and  $\text{Fe}_3\text{O}_4$  layers becomes negligible for  $t_{\text{Cu}}=10$  nm due to the short-range nature of exchange interactions. We observed that the switching of the  $\text{Fe}_3\text{O}_4$  layer becomes comparatively sharper and the difference in coercivity of the two magnetic layers manifests itself in the form of an antiparallel configuration of the  $\text{Ni}_{80}\text{Fe}_{20}$  and  $\text{Fe}_3\text{O}_4$  layers at low magnetic fields. When  $t_{\text{Cu}}$  is further increased to 30 nm, the two magnetic layers are effectively decoupled. In the absence of any coupling effect, the magnetization reversal of the  $\text{Ni}_{80}\text{Fe}_{20}$  and  $\text{Fe}_3\text{O}_4$  layers occurs independently as clearly evident in the form of two sharp switching fields.

In order to extract the contribution of GMR effect from the MR curves, we have averaged the longitudinal and transverse MR curves so as to cancel the AMR effect as suggested in Ref. 16. Shown in Fig. 3 are the GMR curves as a function of  $t_{\text{Cu}}$ . This GMR effect is due to spin-dependent scattering at

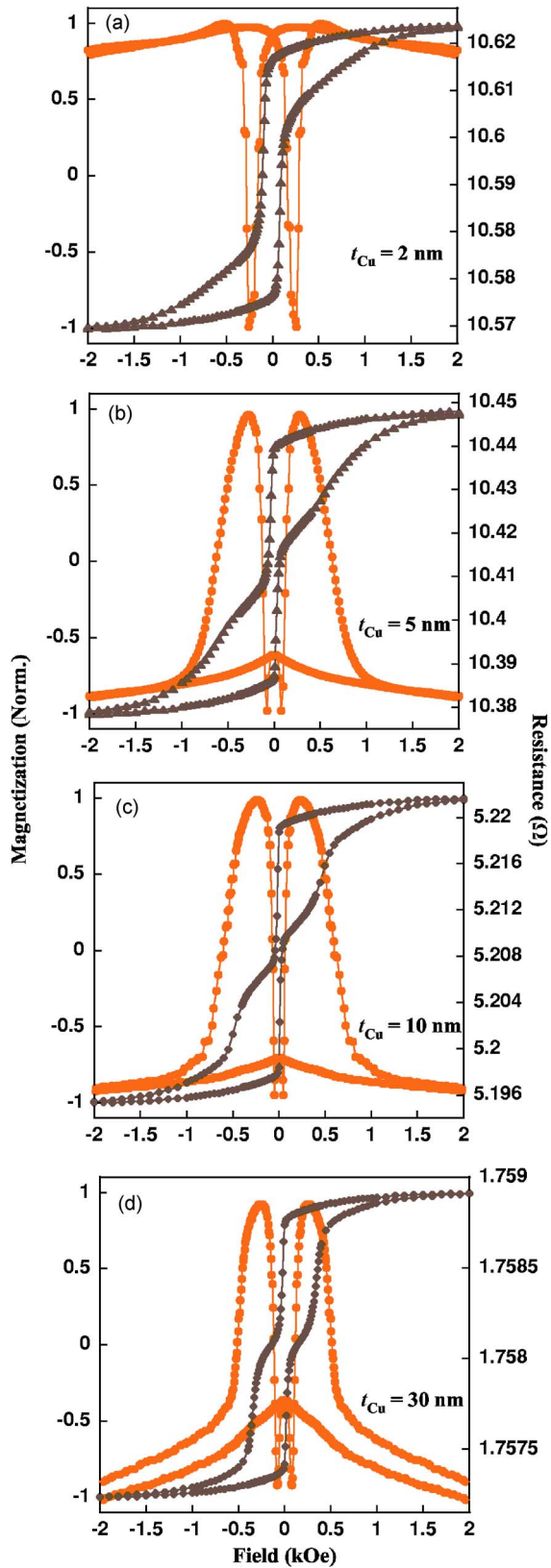


FIG. 2. (Color online). Normalized in-plane magnetization curves ( $\blacktriangle$ ) and longitudinal magnetoresistance curves ( $\bullet$ ) measured at 300 K for  $\text{Fe}_3\text{O}_4$  (60 nm)/Cu ( $t_{\text{Cu}}$ )/ $\text{Ni}_{80}\text{Fe}_{20}$  (15 nm) spin valve structures as a function of  $t_{\text{Cu}}$ .

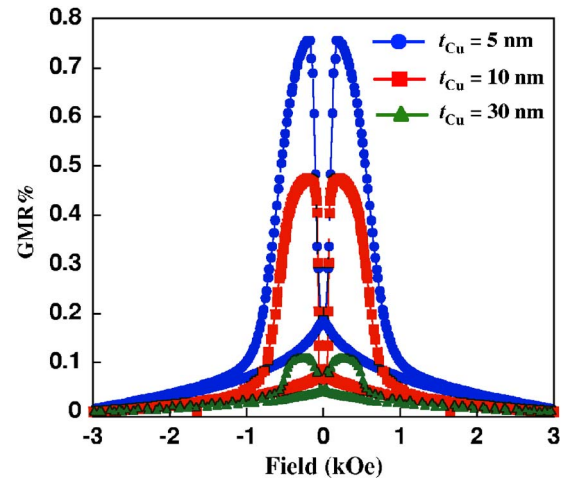


FIG. 3. (Color online). GMR curves measured at 300 K for  $\text{Fe}_3\text{O}_4$  (60 nm)/Cu ( $t_{\text{Cu}}$ )/ $\text{Ni}_{80}\text{Fe}_{20}$  (15 nm) spin valve structures as a function of  $t_{\text{Cu}}$ .

the interface between the magnetic layers and the nonmagnetic Cu spacer layer. We note that the resistance of the spin valve structure at room temperature is about 10.4  $\Omega$  for  $t_{\text{Cu}} = 5$  nm. It decreases to 5.2  $\Omega$  for  $t_{\text{Cu}} = 10$  nm and about 1.75  $\Omega$  for  $t_{\text{Cu}} = 30$  nm. The resistance of the  $\text{Fe}_3\text{O}_4$  layer at room temperature is about two orders of magnitude higher than the entire spin valve structure. Hence, it can be concluded that most of the electrons are confined in the metallic spacer layer and the GMR effect is only due to spin-dependent reflection of electrons at the interfaces between the  $\text{Ni}_{80}\text{Fe}_{20}$  and  $\text{Fe}_3\text{O}_4$  layers and the Cu spacer layer. We also observe that the GMR ratio decreases monotonically with increasing  $t_{\text{Cu}}$ . This decrease in GMR ratio with increasing  $t_{\text{Cu}}$  also confirms that the GMR effect in our spin valve structure is an interface phenomenon rather than a bulk one. The decrease of GMR ratio with increasing Cu spacer layer thickness may be attributed to two main factors, namely; increase in current shunting effects through the bulk of the Cu spacer layer away from the interfacial regions, and a decrease in the probability of spin polarized electrons crossing the Cu spacer layer without scattering, with increasing  $t_{\text{Cu}}$ .<sup>16</sup>

Another characteristic feature of the GMR curves is a progressive evolution in the sharpness of the peaks with increasing  $t_{\text{Cu}}$ . The sharpness of the peaks represents the stiffness of the spin valve structure for holding the antiparallel alignment of the  $\text{Ni}_{80}\text{Fe}_{20}$  and  $\text{Fe}_3\text{O}_4$  layers during magnetization reversal. We observed that the peaks become flatter and wider as  $t_{\text{Cu}}$  is increased from 5 nm to 30 nm. This observation may be attributed to an increased stability of the antiparallel alignment between the  $\text{Ni}_{80}\text{Fe}_{20}$  and  $\text{Fe}_3\text{O}_4$  layers with increasing  $t_{\text{Cu}}$ . It should be also noted that the overall GMR effect in our spin valve structures may be reduced due to the presence of so-called antiphase boundaries (APB's), which are naturally occurring growth defects in  $\text{Fe}_3\text{O}_4$ . The magnetic coupling across a large fraction of these APB's is antiferromagnetic (AF).  $\text{Fe}_3\text{O}_4$  films can be thus described as a linear chain of ferromagnetic domains that are AF coupled at atomically sharp interfaces.<sup>17</sup> Hence, it is difficult to satu-



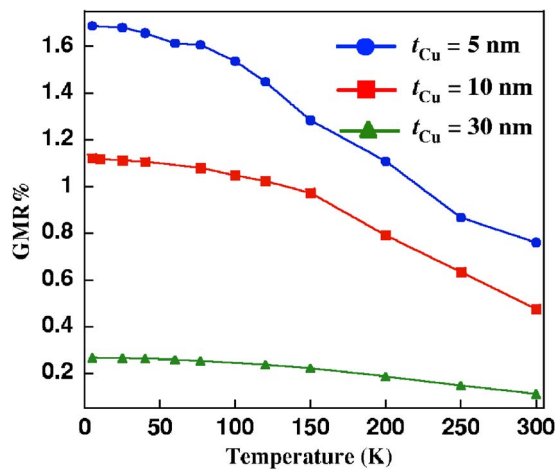


FIG. 4. (Color online). GMR ratio measured as a function of temperature for  $t_{Cu}=5$  nm, 10 nm and 30 nm, respectively.

rate  $Fe_3O_4$  films even in large magnetic fields. Consequently, a complete antiparallel configuration of the  $Fe_3O_4$  and  $Ni_{80}Fe_{20}$  layers cannot be attained and this could reduce the GMR effect drastically.

In order to understand the dependence of GMR ratio on temperature, we have systematically measured the MR curves for our spin valve structures as a function of Cu spacer layer thickness in the temperature range  $5\text{ K} \leq T \leq 300\text{ K}$ . Shown in Fig. 4 is GMR ratio as a function of temperature for  $t_{Cu}$  varying from 5 nm to 30 nm. We observed that the GMR ratio decreases monotonically with increasing temperature for each  $t_{Cu}$ . The decrease in GMR ratio with increasing temperature for our spin valve structure may

be attributed to various possible mechanisms. First, enhanced electron-magnon interaction at higher temperatures will lead to increased spin flip scattering at the interfaces.<sup>9</sup> Moreover, such an electron-magnon interaction may also cause spin mixing, which is detrimental to the GMR effect.<sup>18</sup> Second, with increasing temperature, thermally excited spin waves will reduce the net magnetization, which in turn suppresses the GMR effect.<sup>19</sup> These factors reduce the relative contribution of spin-dependent scattering and hence result in a decrease of GMR ratio with increasing temperature. The GMR ratio is also strongly dependent on the spin polarization ( $P$ ) of the  $Fe_3O_4$  layer which decreases rapidly with increasing temperature due to finite-temperature spin disorder, thermally activated spin mixing and magnon and phonon effects.<sup>20</sup>

In summary, we have presented a systematic study of the magnetization reversal and magnetoresistance behavior of  $Fe_3O_4/Cu(t_{Cu})/Ni_{80}Fe_{20}$  spin valve structures as a function of Cu spacer layer thickness at various temperatures. We observed that for  $t_{Cu}=2$  nm, the  $Ni_{80}Fe_{20}$  and  $Fe_3O_4$  layers are strongly exchange coupled resulting in AMR effect dominating the transport properties of the spin valve structure. For  $t_{Cu} \geq 5$  nm, interlayer exchange coupling decreases rapidly, and the transport properties are dominated by GMR effect. For all temperatures measured, the GMR ratio decreases with increasing  $t_{Cu}$  due to enhanced current shunting and scattering effects.

This work was supported by National University of Singapore (NUS) Grant No. R263-000-283-112. One of the authors (D.T.) would also like to thank NUS for his research scholarship.

\*Corresponding author. Email address: eleaao@nus.edu.sg

<sup>1</sup>M. N. Baibich, J. M. Broto, A. Fert, F. Nguyen Van Dau, F. Petroff, P. Etienne, G. Creuzet, A. Friederich, and J. Chazelas, *Phys. Rev. Lett.* **61**, 2472 (1998).

<sup>2</sup>K. Matsuyama, *J. Magn. Soc. Jpn.* **25**, 51 (2001).

<sup>3</sup>R. A. de Groot, F. M. Mueller, P. G. van Engen, and K. H. J. Buschow, *Phys. Rev. Lett.* **50**, 2024 (1983).

<sup>4</sup>R. A. de Groot and K. H. J. Buschow, *J. Magn. Magn. Mater.* **54-57**, 1377 (1986).

<sup>5</sup>M. Pénicaud, B. Siberchicot, C. B. Sommers, and J. Kübler, *J. Magn. Magn. Mater.* **103**, 212 (1992).

<sup>6</sup>A. Kida, C. Yamamoto, M. Doi, H. Asano, and M. Matsui, *J. Magn. Magn. Mater.* **272-276**, e1559 (2004).

<sup>7</sup>E. Snoeck, Ch. Gatel, R. Serra, G. BenAssayag, J.-B. Moussy, A. M. Bataille, M. Pannetier, and M. Gautier-Soyer, *Phys. Rev. B* **73**, 104434 (2006).

<sup>8</sup>E. Snoeck, Ch. Gatel, R. Serra, J. C. Ousset, J.-B. Moussy, A. M. Bataille, M. Pannetier, and M. Gautier-Soyer, *Mater. Sci. Eng., B* **126**, 120 (2006).

<sup>9</sup>S. van Dijken, X. Fain, S. M. Watts, and J. M. D. Coey, *Phys. Rev. B* **70**, 052409 (2004).

<sup>10</sup>S. van Dijken, X. Fain, S. M. Watts, K. Nakajima, and J. M. D.

Coey, *J. Magn. Magn. Mater.* **280**, 322 (2004).

<sup>11</sup>H. Takahashi, S. Soeya, J. Hayakawa, K. Ito, A. Aida, C. Yamamoto, H. Asano, and M. Matsui, *J. Appl. Phys.* **93**, 8029 (2003).

<sup>12</sup>C. Park, Y. Shi, Y. Peng, K. Barmak, J.-G. Zhu, D. E. Laughlin, and R. M. White, *IEEE Trans. Magn.* **39**, 2806 (2003).

<sup>13</sup>P. A. A. van der Heijden, P. J. H. Bloemen, J. M. Metselaar, R. M. Wolf, J. M. Gaines, J. T. W. M. van Eemeren, P. J. van der Zaag, and W. J. M. de Jonge, *Phys. Rev. B* **55**, 11569 (1997).

<sup>14</sup>Th. G. S. M. Rijks, R. Coehoorn, J. T. F. Daemon, and W. J. M. de Jonge, *J. Appl. Phys.* **76**, 1092 (1994).

<sup>15</sup>T. R. McGuire and R. I. Potter, *IEEE Trans. Magn.* **11**, 1018 (1975).

<sup>16</sup>Th. G. S. M. Rijks, R. Coehoorn, M. J. M. de Jong, and W. J. M. de Jonge, *Phys. Rev. B* **51**, 283 (1995).

<sup>17</sup>J.-B. Moussy, S. Gota, A. Bataille, M.-J. Guittet, M. Gautier-Soyer, F. Delille, B. Dieny, F. Ott, T. D. Doan, P. Warin, P. Bayle-Guillemaud, C. Gatel, and E. Snoeck, *Phys. Rev. B* **70**, 174448 (2004).

<sup>18</sup>J. L. Duvail, A. Fert, L. G. Pereira, and D. K. Lottis, *J. Appl. Phys.* **75**, 7070 (1994).

<sup>19</sup>J.-Q. Wang and G. Xiao, *Phys. Rev. B* **50**, 3423 (1994).

<sup>20</sup>P. A. Dowben and R. Skomski, *J. Appl. Phys.* **95**, 7453 (2004).